

Characterization of 3 mm Glass Electrodes and Development of RPC Detectors for *INO – ICAL* Experiment

Daljeet Kaur, Ashok Kumar, Ankit Gaur, Purnendu Kumar,
Md. Hasbuddin, Swati Mishra, Praveen Kumar, Md. Naimuddin*

Department of Physics and Astrophysics, University of Delhi,
Delhi 110007, India.

December 17, 2014

Abstract

India-based Neutrino Observatory (INO) is a multi-institutional facility, planned to be built up in South India. The INO facility will host a 51 kton magnetized Iron CALorimeter (ICAL) detector to study atmospheric muon neutrinos. Iron plates have been chosen as the target material whereas Resistive Plate Chambers (RPCs) have been chosen as the active detector element for the ICAL experiment. Due to the large number of RPCs needed ($\sim 28,000$ of $2\text{ m} \times 2\text{ m}$ in size) for ICAL experiment and for the long lifetime of the experiment, it is necessary to perform a detailed *R&D* such that each and every parameter of the detector performance can be optimized to improve the physics output. In this paper, we report on the detailed material and electrical properties studies for various types of glass electrodes available locally. We also report on the performance studies carried out on the RPCs made with these electrodes as well as the effect of gas composition and environmental temperature on the detector performance. We also lay emphasis on the usage of materials for RPC electrodes and the suitable environmental conditions applicable for operating the RPC detector for optimal physics output at INO-ICAL experiment.

Keywords: INO, ICAL, RPC, GLASS

*Corresponding author: nayeem@cern.ch

1 Introduction

The India-based Neutrino Observatory (INO) [1] is a multi-institutional collaboration aimed at building a world-class underground laboratory with an all around rock cover of approximately 1 km for non-accelerator based high energy and nuclear physics experiments. It will be a multi-experiment facility and one of the experiments will be Iron CALorimeter (ICAL). The ICAL detector will have modular structure having three modules with each module weighing about 17 ktons and $16\text{ m} \times 16\text{ m} \times 14.5\text{ m}$ in dimension. The entire detector will be magnetized using a magnetic field of around 1.5 Tesla to detect the charge and momenta of particles passing through it. The primary goal of INO-ICAL is to study the atmospheric muon neutrinos. Neutrinos are fundamental particles belonging to the lepton family in the standard model of particle physics. They come in three flavours, one associated with electrons and the others with their heavier partners, the muons and the taus. According to standard model of particle physics neutrinos are massless. However, recent experiments [2]-[26] indicate that neutrinos have finite but small masses that are yet to be precisely measured. Their flavours also changes as they travel, which is known as flavour oscillation. Determination of neutrino masses and mixing parameters is one of the unresolved problems in physics today. The INO-ICAL experiment with its massive magnetized detector will be able to shed light on this issue by measuring the atmospheric oscillation parameters and neutrino mass hierarchy. In order to make these measurements, INO-ICAL needs a robust detector system through which the muons generated due to the interaction of neutrinos with the target material in ICAL can be detected easily. The Resistive Plate Chamber (RPC) detectors are one such detector which can be used as an active detector element in INO-ICAL experiment.

2 Resistive Plate Chamber Detector

The high energy and astroparticle physics experiments generally require detectors which are stable, having long lifetime and cover large detection area. The RPC detector [27, 28], is one such gaseous detector which was pioneered during 1980s. The RPCs detectors are made up from two high resistive parallel plates with uniform graphite coating on opposite sides, generating a uniform electric field when a bias voltage is applied on the two plates. These are rugged, low cost and highly efficient detectors which have their usage in various high energy, nuclear and astroparticle physics experiments as well as applications in imaging and other fields. The main features of RPC detectors are their large pulse heights, excellent timing resolution better than few nanoseconds, high detection efficiency for minimum ionising particles and low cost per unit area. Their excellent time resolution, possibility of high granularity readout and good detection efficiency make them ideal for the development of fast, efficient and robust triggering system for muons over large areas in hybrid detectors [29]. These detectors are also used for time of flight measurements [28, 30] and for tracking in multilayer configurations in BELLE [31], BaBar [32], L3 [33], OPERA [34], and the LHC experiments (ALICE, ATLAS and CMS) [35] - [37]. RPC detectors has the ability to provide two dimensional readout at a time. These are also very simple to construct and are almost free from damaging discharges.

In INO-ICAL experiment, RPCs are proposed to be used as active detector element. Their high gain, simple design and affordable cost makes it favourite to construct about 28,000 detectors of dimension, $2\text{ m} \times 2\text{ m}$, that INO-ICAL need. The experiment is planned to operate at least for 20 years and may also be upgraded to 100 kton in later phases. Because of the huge number of detectors required for INO-ICAL and keeping in mind the long life span of the experiment, it is pertinent to perform a vigorous *R&D* to carefully optimize the various detector design and operational parameters like the electrode material, gas composition, operational conditions, etc. to exploit fully all the advantages of the RPC detectors. Keeping in view the huge quantity of glasses required and the complexity involved in its long distance transportation, we decided to pursue our *R&D* on the glasses available locally. The earlier *R&D* performed for INO-ICAL glass RPCs were for 2 mm thick glasses only and was also limited in its scope [38, 39]. Due to handling issues and shear stress problems involved in the large size detectors, INO-ICAL collaboration has decided to use 3 mm thick glasses for constructing the RPCs, therefore, all the results reported in this paper are for 3 mm thick glasses.

2.1 Electrodes choice for RPC

In RPC detectors, material properties of electrodes and environmental factors play a significant role in detector working. The electrodes are usually made up of float glass or bakelite and the choice of it depends on the expected event rate. Electrode material plays an important role in the functioning of the RPC detectors, so its selection must be done carefully. Typically, the electrodes should have high resistivity to

control counting rate and preventing spread of discharge throughout the entire gas volume [27, 40, 41]. It must also have uniform surface to avoid localization of excess charge and to prevent alternating leakage path during the avalanche process.

Since INO-ICAL experiment is going to construct huge number of RPCs which in turn requires a large amount of the electrode's material, therefore, one factor that also becomes very important in the selection of electrodes is the ease of availability of it at a reasonable cost. We selected three types of glasses *viz.*, Saint Gobain, Asahi and Modi which are easily and readily available in the local market at a reasonable price for our *R&D*.

We performed the bulk resistivity and surface resistivity measurements of the electrodes to determine their electrical properties. The uneven surface texture of electrodes surface properties gives a profound effect on the detector performance because of the increase in dark current, counting rate and thus influencing the efficiency of the detector. For the purpose of determining the surface properties we performed Scanning Electron Microscopy (SEM) and Atomic Force Microscopy (AFM) analysis.

2.1.1 Bulk and Surface Resistivity

The bulk resistivity of the electrode material of the RPC was determined through the measurement of current through the glass for a given bias voltage. The bulk resistivity has been measured using the glass samples cut into 3 cm \times 3 cm of size. Two cables were soldered on two different copper plates which are connected to the CAEN N471A high voltage power supply. The copper plates were placed on the adjacent flat surfaces of the glass sample and a bias voltage was applied across it. The current measured by the inbuilt ammeter inside CAEN N471A was noted down as a function of the applied voltage. Fig. 1 shows the bulk resistivity of the three types of glasses as a function of the applied bias voltage. The Saint Gobain glass was found to have the maximum bulk resistivity among all the three samples. In the operating region of around 6 kV, the Saint Gobain bulk resistivity is of the order $5 \times 10^{12} \Omega\text{-cm}$ on average. Asahi and Modi were found to be having similar bulk resistivity and is approximately $1.5 \times 10^{12} \Omega\text{-cm}$ in the operating region around 5 kV. The bulk resistivity measurements were repeated many times and the results varied within less than 5% from its mean value.

The circuit for surface resistivity measurement is made with two brass bars with soft padded conducting edges at the bottom, which were placed on the test sample. The length of the brass bars and their separation were kept at 5 cm. A DC bias voltage was applied on the jig and the leakage current across the terminals of the jig through the sample was measured. A total of 10 measurement points were taken on each plate to obtain a fine binning. Also, the measurements were repeated many times for the same point and the results were found to be reproducible within 8% uncertainty from the mean value. Fig. 2 shows the average surface resistivity measurements of the three glasses. It can be seen from this figure that the surface resistivity of the Asahi glass is approximately constant over most of surface area, whereas there are significant variations in the surface resistivity distribution of the Saint Gobain glass. The Modi glass has even wider surface resistivity variations. From the scale of surface resistivity variations of the three glasses, it can be concluded that the Asahi is having the smoothest surface of all followed by Saint Gobain and Modi respectively [42]. The measurements of bulk and surface resistivity were performed under normal pressure, relative humidity maintained between 45% to 50% and temperature between 20°C to 21°C.

2.1.2 Surface Properties

The rough inner surface of the electrodes may cause wide variation in the electric field inside the RPC. Due to rough surface the sharp uneven edges in the surface morphological structure causes the electric field inside the RPC to vary significantly. Rough surface is very sensitive to the field emission which is a source of high dark current and high counting rates. Therefore, it is very important to perform a panoramic study of surface roughness for the efficient operation of the RPC. We determined the roughness (or smoothness) of the electrodes surface through the AFM scanning. The average roughness is defined as:

$$R_{av} = \sqrt{\frac{\sum_i (t_{av} - t_i)^2}{N}} \quad (1)$$

where, t_{av} is the average height, t_i is the individual measured height as shown in Fig. 3, and N is the number of data points scanned on the surface. The average roughness of 1.28 ± 0.33 nm, 2.00 ± 0.96 nm and 2.81 ± 1.56 nm was found for Asahi, Saint Gobain and Modi respectively. The errors on the roughness are standard errors

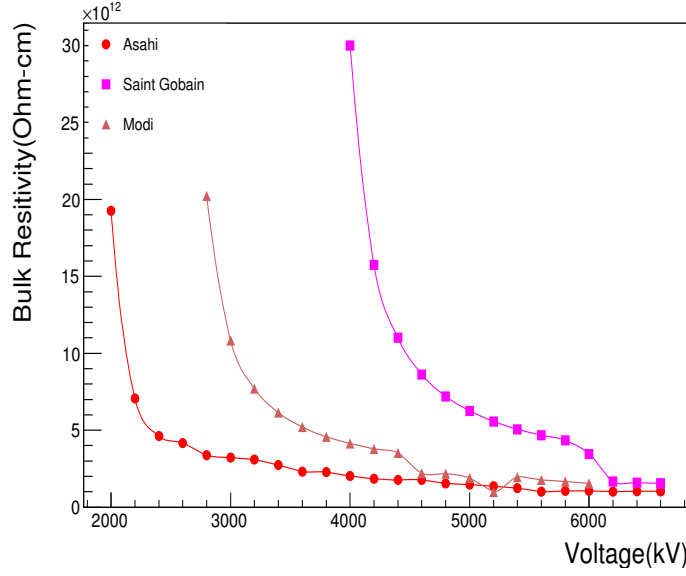


Figure 1: Bulk Resistivity of all the three types of glasses in Ω -cm as a function of the applied voltage.

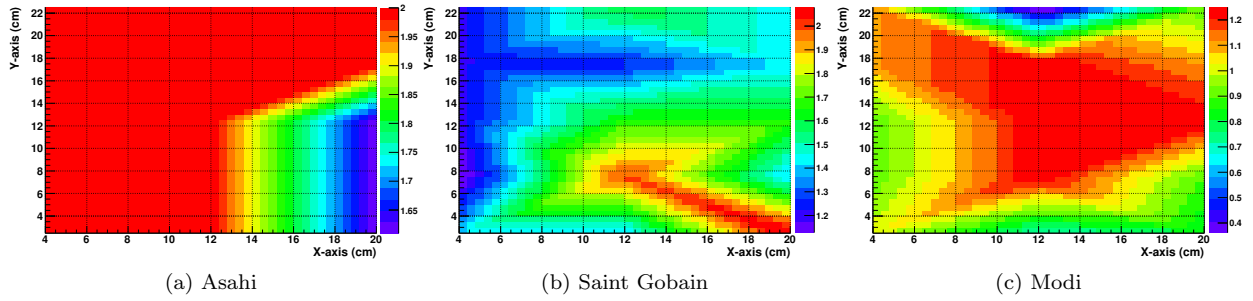


Figure 2: Surface Resistivity for all the three glasses. The X and Y axes are the length and breadth in centimeters of the glass plates whose surface resistivity was measured. The intensity of the colours indicates the value of the surface resistivity in $10^{11} \Omega/\square$ and the variation in colours represents the variation in the surface resistivity at different points across the glass plate.

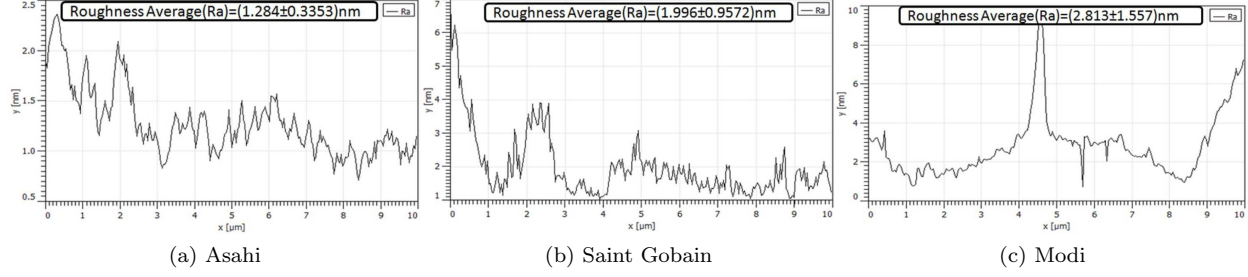


Figure 3: Atomic Force Microscopy scans for the three glass samples. The X-axis shows the scanned length of the glass sample in μm , and Y-axis shows the variation in the surface roughness (or smoothness) in nm

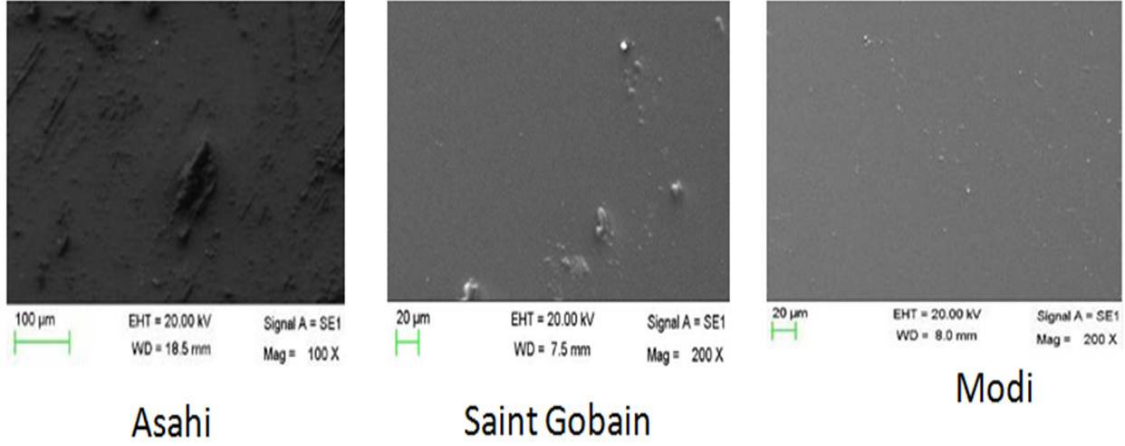


Figure 4: Electron Microscopy scans for the three glass samples.

on the mean value. The SEM images for the three glasses are shown in Fig. 4. The SEM images were taken from ZEISS MA15 instrument at 20 kV using common electron beam. The AFM and SEM measurements alone are not conclusive enough to declare any sample as smoother than other with high confidence, however, after taking into account the surface resistivity results together with the AFM and SEM measurements, we can conclude that, at least, qualitatively Asahi glass appears to have the smoothest surface of all. Since these results were not conclusive enough quantitatively to reject any of the three glass samples at this stage, we proceeded to fabricate the RPCs using all the three samples to perform the characterization studies.

To confirm that the glasses we have selected are amorphous in nature, we performed an X-ray diffractometer scan with REGAKU D-2000 instrument with acceleration voltage of 40 kV, current of 100 mA, and $\text{Cu} - K\alpha$ as an X-ray. The XRD study confirms molten glassy type matrix for all the samples. We also performed the study for the determination of the composition percentage of elements present in electrode samples. Carbon, Sodium, Magnesium, Aluminium, Silicon, Calcium, Oxygen and Tin have been found in different quantity in the three glasses. The detailed composition is given in Table 1. It can be seen from the table that Saint Gobain glass has no Carbon component whereas Asahi and Modi have 4.89% and 6.68% Carbon component respectively. Since Carbon is a conducting element so absence of it from the Saint Gobain glass could be one of the reasons for its high bulk resistivity compared to Asahi and Modi.

2.2 Construction of RPC Chambers

Using three different types of glasses mentioned in the previous section, we fabricated small prototypes of size $30 \text{ cm} \times 30 \text{ cm}$ RPCs in our lab. Each glass plate electrode was chosen to be 3 mm and coated with a conductive layer of graphite on the outer surface. Buttons made up of polycarbonate material were glued on the electrode surface for the uniform gap separation of 2 mm between the two electrode plates. The gas gaps were sealed using polycarbonate side spacers from all sides. A gas inlet and a gas outlet nozzles made up of polycarbonate were glued on the diagonally opposite corners of the RPCs. The pickup panel consisted of honey comb panels with copper strips of width 2.80 cm placed above and below the electrodes.

Serial No.	Element Name	Percentage of Elements		
		Asahi	Saint Gobain	Modi
1	C	4.89	-	6.68
2	Na	6.89	8.22	6.34
3	Mg	1.79	1.85	1.55
4	Al	0.32	0.27	0.31
5	Si	21.7	24.56	20.44
6	Ca	2.71	3.32	2.45
7	O	61.67	59.97	61.99
8	Sn	-	0.58	-

Table 1: Element composition in the three glass samples in atomic weight percentage.

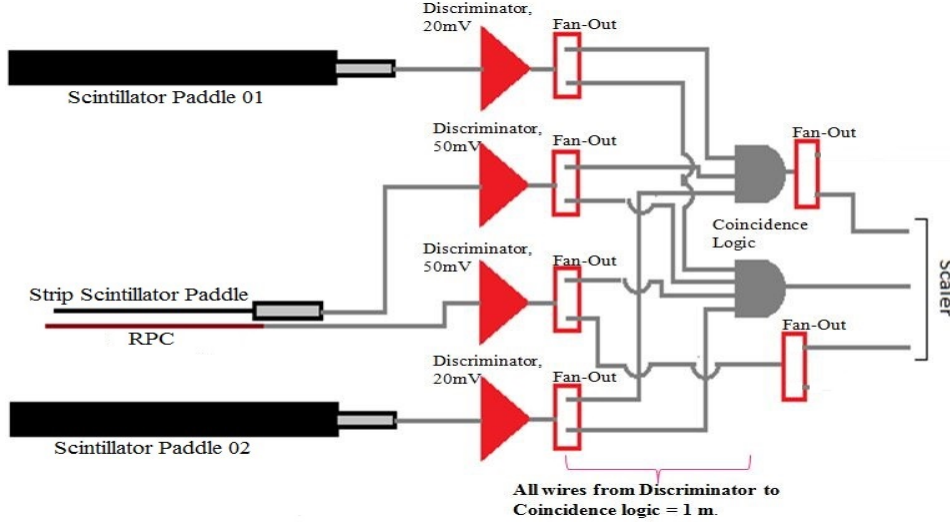


Figure 5: Setup for the muon telescope with DAQ

After assembling the detector, we performed the leak test using manometer technique by measuring the pressure difference (water level difference in both arms) with respect to time.

3 Detector Characterization

To characterize the performance of the RPCs made from the three types of glasses, we performed the efficiency, noise rate and leakage current measurements. A muon telescope consisting of three scintillator detectors being connected with the NIM/VME Data Acquisition system (DAQ) was used for conducting these measurements. The detector to be characterized is interleaved in between the scintillator detectors and readout by the DAQ system as shown in Fig. 5. All the measurements reported in the next sections were performed at the normal pressure, relative humidity varying between 45% to 50% and temperature varying between 20°C to 21°C except for the temperature variation study reported in sec. 3.3.

The RPCs are characterized for efficiency, leakage current and noise rate under different environmental and running conditions. We characterize the RPCs for various gas compositions, temperatures and thresholds to obtain the optimum parameters to maximize the detector performance.

3.1 Variation of Gas Mixture Composition

The RPC detector uses different composition of gas mixtures to optimize the efficiency and longevity of the detectors. However, it has been found that choosing the best composition of gases is not an easy job and depends on many factors, like the material of the electrodes, the readout mode, the environment, etc. Many of the standard gas mixtures have unpleasant features such as flammability, formation of unwanted elements, etc. A large number of studies have already been performed in this direction [43]-[47]. Therefore, it is very

important to make an extensive study in order to choose the right composition of gases for the INO RPC detectors. The RPCs were tested in avalanche mode with four different gas mixture compositions as follows:

1. First Composition : $R134a$ (95.0%), C_4H_{10} (5.0%), SF_6 (0.0%).
2. Second Composition : $R134a$ (90.0%), C_4H_{10} (10.0%), SF_6 (0.0%).
3. Third Composition : $R134a$ (95.0%), C_4H_{10} (4.5%), SF_6 (0.5%).
4. Fourth Composition : $R134a$ (90.0%), C_4H_{10} (9.0%), SF_6 (1.0%).

The flow rate was kept fixed at 10 SCCM (Standard Cubic Centimeter per Minute) for all the compositions. Since the Freon gas is the primary ionising gas so it would not make much sense to reduce the composition of this to a low level, therefore, we varied this between 90 and 95%. The C_4H_{10} is a flammable gas so it would not be advisable to increase its composition to large fraction due to safety reasons, therefore, we varied this between 4.5 to 10%. The SF_6 gas is used as a quenching gas therefore, its composition has been kept low and varied from 0 to 1%. For all the above compositions, we measured the efficiency, noise rate and leakage current of the RPCs made from all the three types of the glasses. Fig. 6 shows the leakage current, efficiency, and noise rate for the first gas composition. Fig. 7, Fig. 8 and Fig. 9 shows the same quantities for the second, third and fourth gas compositions respectively. From these figures it can be seen that the efficiencies for all these gas composition are similar for all the types of the glasses and is above 95%. Noise rate as expected is maximum in the absence of SF_6 and decreases as we increase the SF_6 fraction. The noise rate is maximum for Modi and minimum for Asahi. Leakage current is much higher for Modi compared to Asahi and Saint Gobain which have reasonable values. These observations are consistent with the roughness measurement reported in section 2.1.2, where we found Modi glass having the most rough surface while Asahi having the least rough surface with Saint Gobain in between.

3.2 Variation of Thresholds

The threshold value set in the discriminator circuit to reduce the spurious count rate may also affect the performance of the detector. In order to see the effect of this we varied the thresholds values for the RPC and scintillator paddles and measured the efficiencies and noise rates. Fig. 10 shows the effect of threshold variation on the efficiency and noise rates for Asahi glass RPC. We did not observe much dependence in efficiency between the threshold of 30 mV and 50 mV, whereas, the noise rate decreases as we increase the threshold value from 30 mV to 50 mV. However, further increasing the threshold value up to 70 mV did not decrease the count rate much, so we fixed the threshold value of 50 mV for further studies.

3.3 Variation of environmental Temperature

Environmental conditions like temperature and moisture also affects the performance of the RPC detectors, so it is very important to find out the suitable environmental conditions to operate the RPC in order to optimize the performance. We varied the temperature from 18° C to 24°C and measured the efficiency, noise rate and leakage current for the RPCs made up from all the three types of glasses. Fig. 11 shows the effect of temperature variation on the efficiency, current and noise rate for the RPC made up of Asahi glass. Other two glasses also show the similar characteristics.

4 Results and Conclusions

The INO-ICAL experiment will be using approximately 28,000 RPCs of size 2 m × 2 m. Before we embark up on building such a large amount of RPCs it is important to perform a thorough *R&D* on all aspects of the detector performance before freezing various parameters. We choose three types of glasses available in the local market, *viz.* Asahi, Saint Gobain and Modi. We performed various studies to assess the electrical properties of these three types of glasses. From our studies, we conclude that qualitatively Asahi is better than Saint Gobain and Modi in terms of smoothness. Saint Gobain is best in terms of bulk resistivity.

From performance studies, we find that all the three glasses gives almost similar efficiencies under all conditions. The threshold voltage for Saint Gobain is higher than others and the reason for this could be the higher bulk resistivity of the Saint Gobain glass. Saint Gobain shows lowest count rate for all the gas compositions. Leakage current is lowest for Saint Gobain for the first three gas compositions while Asahi

shows the lowest current for the fourth gas composition. However, at lower bias voltages large fluctuation in the current was observed. The error on the current measurement is $2\% \pm 9$ nA, so the fluctuation in current measurements at low voltages are consistent with each other within errors. From our gas mixture composition studies, we find that the efficiency is not much dependent on the gas composition. The third composition of *R134a* (95.0%), *C₄H₁₀* (4.5%), *SF₆* (0.5%) is found to be giving the lowest noise rate and least current, therefore, we used this composition to perform further measurements. The study on variation of temperature shows that with increase in temperature from 18 to 21 °C, there is not much effect on leakage current and noise rate. But, further increasing the temperature to 24°C, both the leakage current and noise rate increases. It is to be noted, however, that the relative humidity was consistently on the higher side (50%) for the measurements done at the temperatures of 18°C and 24°C whereas it was on the lower side (around 45%) for the measurements performed at the 21°C. We believe this variation in atmospheric relative humidity to be the reason for transition in leakage current and noise rate at 24°C when the humidity is also on the maximum side. We did not find any considerable effect of temperature variation on efficiency.

The discriminator threshold variations show that increasing the threshold from 30 mV to 50 mV decreased the spurious count rate considerably. However, further increasing the threshold from 50 mV to 70 mV did not have any effect on count rate. The efficiency does not depend much on the threshold variation from 30 mV to 50 mV. From this study we conclude that the threshold of 50 mV is a reasonable choice to operate the RPCs.

In conclusion, we found that Saint Gobain and Asahi glasses are best suited for the INO-ICAL RPCs in terms of most of the parameters that we studied. We suggest to operate the RPC under the *R134a* (95.0%), *C₄H₁₀* (4.5%), *SF₆* (0.5%) gas composition and keep the temperature around 20°C in the INO cavern. It is to be noted, however, that all the studies reported in this paper were performed on small prototypes RPCs of size 30 cm × 30 cm. We are in the process of constructing actual size INO-ICAL RPCs to further continue our studies.

5 Acknowledgments

We would like to thank the Department of Science and Technology (DST), India and University of Delhi *R&D* grants for providing the financial support. Daljeet Kaur would like to thank Council of Scientific and Industrial Research (CSIR), India for providing the financial support. We would also like to thank the INO group at Tata Institute of Fundamental Research (TIFR) for providing some of the raw materials for detector construction. Our Sincere thanks to Prof. J. P. Singh of IIT Delhi for his help in getting AFM scans at IIT Delhi.

References

- [1] S. Athar, et al., The Technical Design Report of INO-ICAL Detector (2006).
- [2] S. Abe et al. [KamLAND Collaboration], Phys. Rev. Lett. **100** (2008) 221803.
- [3] Fukuda, Y., et al. Physical Review Letters **81** (8): 15621567 [arXiv:9807003][hep-ex](1998).
- [4] R. Wendell et al. [Super-Kamiokande Collaboration], Phys. Rev. **D 81**, 092004 (2010).
- [5] P. Adamson et al. [MINOS Collaboration], Phys. Lett **110**, 251801 (2013).
- [6] K. Abe et al. (T2K collaboration), Phys. Rev. Lett. **112**, 181801 (2014).
- [7] D. J. Koskinen, Mod. Phys. Lett. **A 26**, 2899 (2011).
- [8] B. T. Cleveland et al., Astrophys. J. 496, 505 (1998).
- [9] F. Kaether, W. Hampel, G. Heusser, J. Kiko, and T. Kirsten, Phys.Lett. B685, 47 (2010).
- [10] J. N. Abdurashitov et al. (SAGE Collaboration), Phys. Rev. C80, 015807 (2009).
- [11] G. Bellini, J. Benziger, D. Bick, S. Bonetti, G. Bonfini, et al., Phys.Rev.Lett. 107, 141302 (2011).
- [12] B. Aharmim et al. (SNO), Phys. Rev. Lett. 101, 111301 (2008).

- [13] B. Aharmim et al. (SNO), Phys. Rev. C **81**, 055504 (2010).
- [14] J. Hosaka et al. (Super-Kamiokande), Phys. Rev. D **73**, 112001 (2006), [arXiv:0508053][hep-ex].
- [15] J. Cravens et al. (Super-Kamiokande Collaboration), Phys.Rev. D **78**, 032002 (2008).
- [16] K. Abe et al. (Super-Kamiokande Collaboration), Phys.Rev. D **83**, 052010 (2011).
- [17] Renshaw (Super-Kamiokande Collaboration) (2014), 1403.4575.
- [18] The Super-Kamiokande Collaboration, Phys. Rev. Lett. **112**, 091805(2014), [arXiv:1312.5176]
- [19] [KamLAND Collaboration] "Precision Measurement of Neutrino Oscillation Parameters with KamLAND", Phys. Rev. Lett. **100**(22) 221803 [arXiv:0801.4589].
- [20] Y. Abe et al. [Double Chooz Collaboration], Phys. Rev.D **86**, 052008 (2012).
- [21] DAYA-BAY Collaboration, F. An et al., Phys. Rev. Lett. **108**, 171803 (2012), [arXiv:1203.1669].
- [22] RENO collaboration, J. Ahn et al., Phys. Rev. Lett. **108**, 191802 (2012),[arXiv:1204.0626].
- [23] P. Adamson et al., Phys.Rev.Lett. **110**, 171801 (2013)
- [24] P. Adamson et al. [MINOS Collaboration], Phys. Lett **110** (2013) 251801.
- [25] K. Abe et al.(T2K collaboration), Phys. Rev. Lett. **112** (2014) 181801.
- [26] F.Capozzi et al., Phys. Rev.D **89** 093018.
- [27] R. Santonico, R. Cardarelli, Nucl. Instr. and Meth. **A 187** (1981) 377.
- [28] R. Santonico, R. Cardarelli, Nucl. Instr. and Meth. **A 263** (1988) 20.
- [29] G. Bencze et al., Nucl. Instr. and Meth. **A 340** (1994) 466.
- [30] A. Blanco et al., Nucl. Instr. and Meth. **A 513** (2003) 8.
- [31] A. Abashian et al., The Belle Detector, Nucl. Instr. and Meth. **A 479** (2002)
- [32] BaBar Collaboration, BaBar Technical Design Report, SLAC Report SLAC-R-95-457 (1995).
- [33] L3 Collaboration, B. Adeva, et al., The construction of L3 experiment, Nucl. Instr. Meth. **A 289** (1990) 35.
- [34] OPERA Collaboration, M. Guler et al., An appearance experiment to search for $\nu_{\mu\mu}-\nu_{\tau\tau}$ oscillations in the CNGS beam: experimental proposal, CERN/SPSC 2000-028 (2000).
- [35] ALICE Collaboration, ALICE Technical Design Report of the time-of-flight system (TOF), CERN-LHCC 2000-12 (2000).
- [36] ATLAS Collaboration, ATLAS muon spectrometer: Technical Design Report, CERN-LHCC 97-22 (1997).
- [37] CMS Collaboration, Technical Proposal, CERN-LHCC-94-38 (1994); CMS Collaboration JINST, **3** (2008) S08004.
- [38] Sarika Bhide, V.M. Datar, Satyajit Jena, S.D. Kalmani, N.K. Mondal, G.K. Padmashree, B. Satyanarayan, R.R. Shinde, P. Verma, Pramana, Journal of Physics **69(6)** (2007) 1015-1023.
- [39] V.M. Datar, Satyajit Jena, S.D. Kalmani, N.K. Mondal, P. Nagaraj, L.V. Reddy, M.Saraf, B. Satyanarayan, R.R. Shinde, P. Verma, Nucl. Instr. and Meth. **602** (2009) 744-748.
- [40] H. Czyrkowski, et al., Nucl. Instr. Meth. **A 419** (1998).
- [41] R. Cardarelli, A. Di Ciaccio and R. Santonico, Nucl. Instr. Meth. **A 333** (1993).
- [42] K. K. Meghna, et al., JINST **7** P10003 (2012).

- [43] A. Mengucci, A. Paoloni, M. Spinetti, L. Votano, Nucl. Instr. Meth. **A 583** (2007) 264-269.
- [44] M. Cwoik, W. Dominik, M. Gorski, J. Krolikowski, Nucl. Instr. Meth. **A 508** (2003) 38-43.
- [45] MA Lie-Hua, et al., Chinese Physics **C 34**(8) 2010, 1116-1121.
- [46] M. Salim, R. Hasan, N. Majumdar, S. Mukhopadhyay, B. Satyanarayana, JINST **7** P11019 (2012).
- [47] K. Abe, et al., Nucl. Instr. Meth. **A 455** (2000) 397-404.

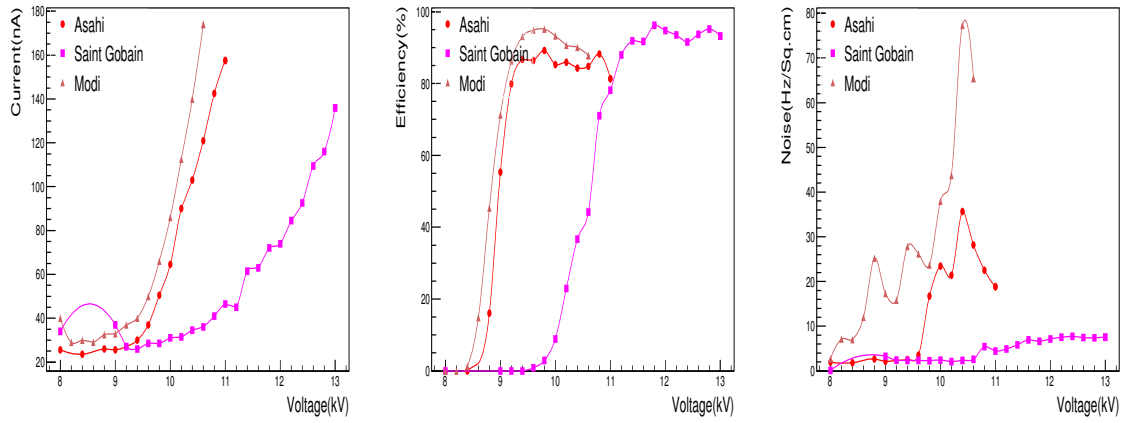


Figure 6: Leakage current, efficiency and Noise rate for the first composition.

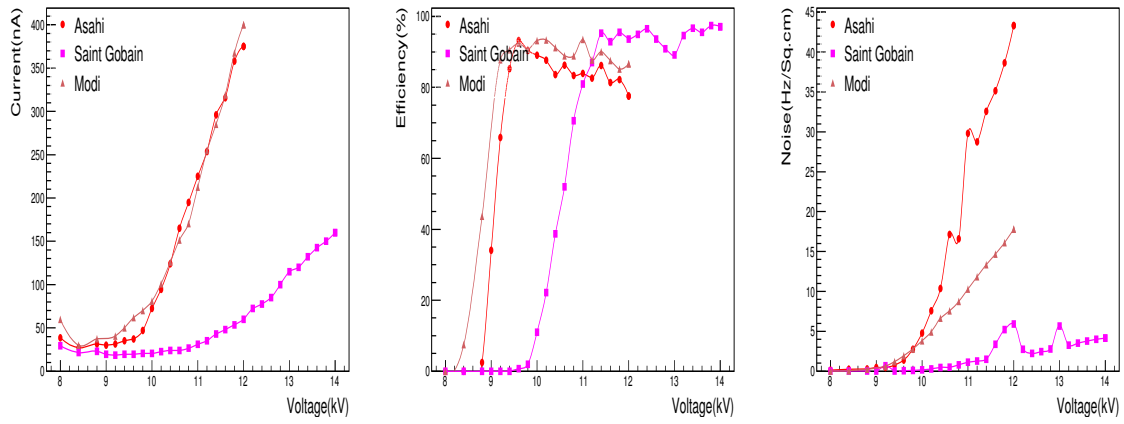


Figure 7: Leakage current, efficiency and Noise rate for the second composition.

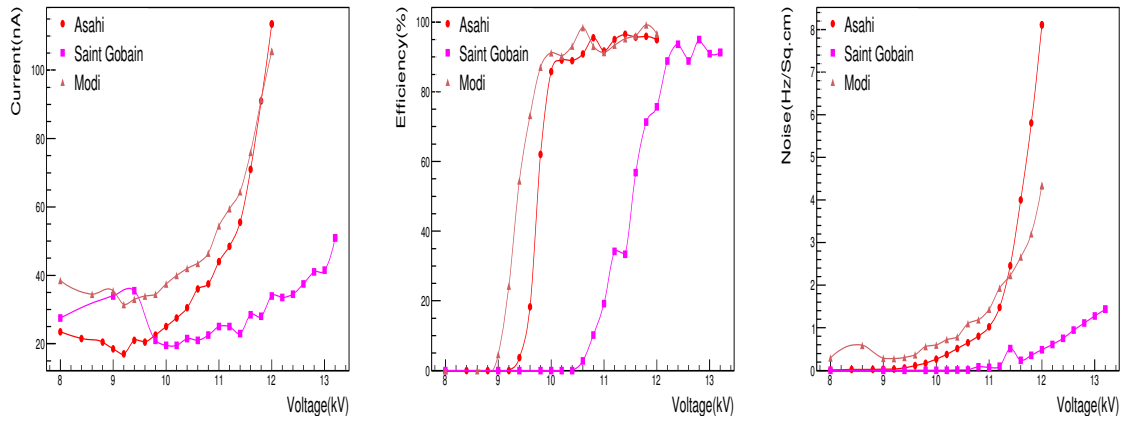


Figure 8: Leakage current, efficiency and Noise rate for the third composition.

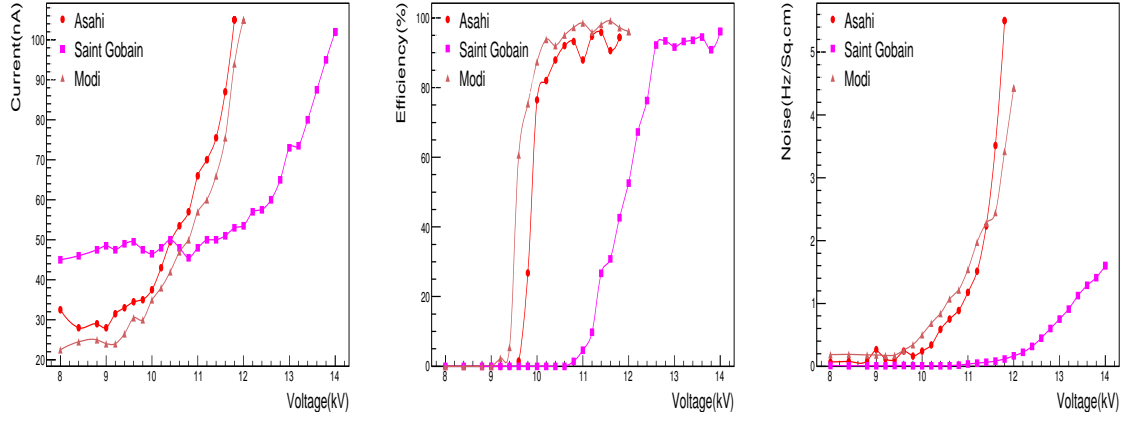


Figure 9: Leakage current, efficiency and Noise rate for the fourth composition.

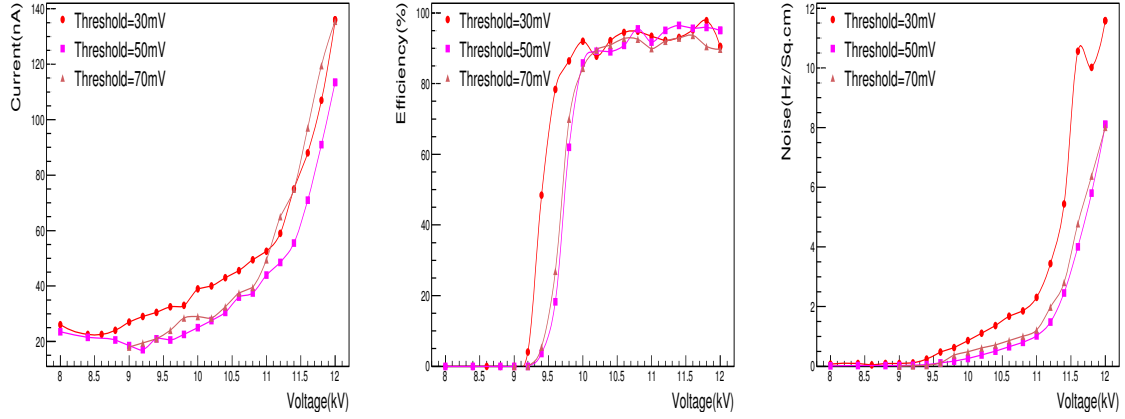


Figure 10: Leakage current, efficiency and Noise rate for Asahi Glass at three different threshold values and with third gas composition

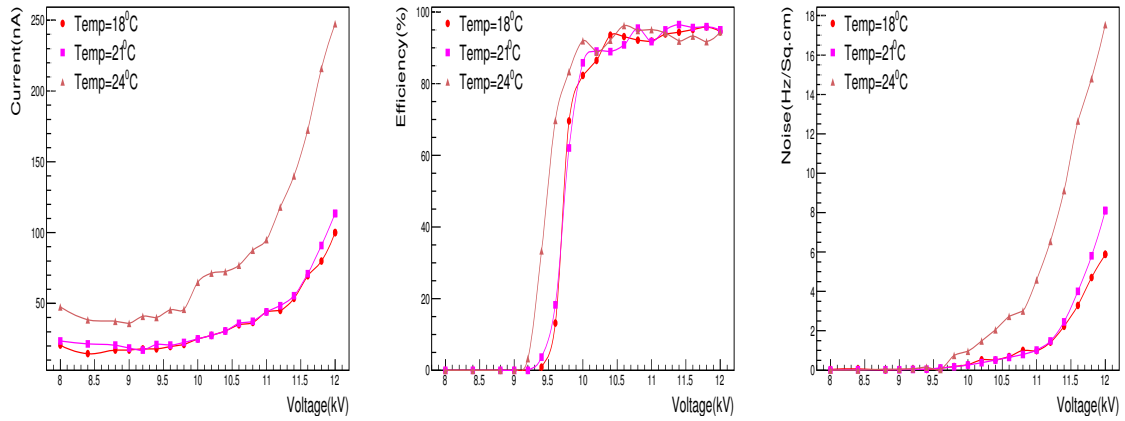


Figure 11: Leakage current, efficiency and noise rate for Asahi Glass at three different temperatures. These measurements are with third gas compositions.